Chemical Engineering Journal 144 (2008) 531–539

Contents lists available at ScienceDirect

Chemical Engineering Journal

journal homepage: www.elsevier.com/locate/cej

RESS process in coating applications in a high pressure fluidized bed environment: Bottom and top spray experiments

S. Rodríguez-Rojo, J. Marienfeld, M.J. Cocero*

High Pressure Processes Group, Department of Chemical Engineering and Environmental Technology, University of Valladolid (Spain), Prado de la Magdalena s/n, 47011 Valladolid, Spain

ARTICLE INFO

Article history:
Received 17 March 2008
Received in revised form 27 July 2008
Accepted 31 July 2008

Keywords:
RESS
Nozzle
Fluidization
Coating
High pressure
Paraffin wax
Solubility

ABSTRACT

Fluidized bed combined with RESS process in supercritical carbon dioxide (SC-CO_2) is a promising technology for coating heat-sensitive materials of high added value. This work presents a study of the most influencing operation parameters (temperature, pressure and flow) of the two steps of the process (saturation and coating).

As a model system, glass beads particles ($d_{p,s}$ = 176 μm) were encapsulated with paraffin (T_m = 52–54 °C). Two different ways of injecting the coating solution of paraffin in the SC-CO_2 in the fluidized bed were tested, bottom and top spray. The operation variables were kept in the following ranges for the saturation step: pressure from 18 to 22 MPa and temperature from 35 to 55 °C. In the coating process the pressure range from 8 to 10 MPa and temperature from 35 to 50 °C. Yields of the global process up to 70% were achieved. SEM-images of the achieved coatings show complete coating films with no agglomeration in the top spray experiments.

1. Introduction

Coating of particles offers various unique advantages and is today a widely used technique in particle processing. Coating can modify physical characteristics of the original material such as hygroscopicity, appearance (color and shape), apparent density, compressibility and mechanical strength [1,2]. Encapsulation can also result in more uniform particle size distribution, smoother surfaces and dust reduction, which improves handling, flowability and further processing [3,4]. Regarding the chemical characteristics, the most important applications of coatings are the protection of unstable ingredients in the particle from external degradation factors such as heat, moisture, air and light [2], and the controlled release of drugs, where the dissolution of an active component is slowed down due to a coating layer and so the release rate to the organism can be adjusted [5]. Most shell materials are natural or synthetic organic polymers, but fats and waxes are also used.

There is no universally accepted size classification of these coated particles or capsules. Commercial micro-capsules typically have a diameter between 3 and 800 μm and contain 10–90 wt.% carrier/core materials [6].

Classic processes for particle coating usually work with organic solvents to bring in the coating substances and use high temperatures to evaporate these solvents (organic phase separation, spray drying, solvent separation and emulsification/solvent evaporation). Both, high temperatures and residuals of organic solvents are problematic in case of drug treatment, since organic solvents might be harmful, not only for the human beings but also for the environment, and many pharmaceutical products are temperature sensible and will suffer from high processing temperatures. Therefore, there has been a continuing growth of interest in replacing conventional organic solvents with environmentally friendly supercritical solvents in encapsulation processes. As a result, particle design has become an important part of supercritical fluids (SCF) applications in pharmaceutics, as well as in food, cosmetics, and several areas of industrial chemistry. The need for high-purity products together with the low cost and easy recoverability of carbon dioxide makes it an attractive solvent in the industrial processing of pharmaceuticals [6].

The applicability of the different techniques for particles generation and coating with SCF depends mainly on the solubility of the coating material in the SCF [6,7], consequently, these precipitation processes can be classified according to the role of the SCF in the process: it can act as a solvent, as in the rapid expansion of supercritical solutions (RESS) process [8]. As an anti-solvent, as in the supercritical anti-solvent processes (SAS) [9]. As a solute, as in the precipitation from gas saturated solution process (PGSS) [10]

* Corresponding author. Tel.: +34 983 42 31 74; fax: +34 983 42 30 13.
E-mail address: mjcocero@iq.uva.es (M.J. Cocero).

1385-8947/$ – see front matter © 2008 Elsevier B.V. All rights reserved.
doi:10.1016/j.cej.2008.07.054

Nomenclature

Ar	Archimedes number
d	diameter (m)
L	length (m)
m	mass (kg)
P	pressure (MPa)
Re	Reynolds number
T	temperature (°C)
u	velocity (ms^{-1})
X	wax loading ($g\,g^{-1}$)

Greek symbols

Δ	difference
ε	porosity
η	yield
μ	viscosity ($kg\,m^{-1}\,s^{-1}$)
ρ	density ($kg\,m^{-3}$)
Φ	sphericity

Indices

m	melting
mf	minimum fluidization
p	particle
s	Sauter diameter or volumen–surface mean diameter

or even as a propeller, as in the supercritical assisted atomization (SAA) process [7].

Besides, there are processes that involve a reaction in supercritical media (H_2O, CO_2 or short chain alcohols) leading to particle formation. These processes are use to synthesize ceramics and metal oxides, generally in the nanoscale, via thermal decomposition of an organic precursor [11].

1.1. RESS applications in coating processes

This work is focused in the application of RESS process to coating where the SFC is the unique solvent. The first to use a RESS process for coating reasons were Debenedetti et al. [12] in 1993, using SC-CO_2 as solvent, while the carrier material was agitated in a stirred tank reactor. Since then, different alternatives have been developed, such as rapid expansion from supercritical solution with a nonsolvent (RESS-N) [13,14]. Because of the low solubility of the most part of polymers in SC-CO_2, cosolvents are used to enhance solubility of the polymer in the supercritical fluid. At atmospheric pressure, these cosolvents are nonsolvents for the polymers, consequently, they do not swell the polymer product during expansion and adhesion is not expected. For polymers, it has been demonstrated that cosolvents that cause a large increases of solubilities in CO_2 need not be good solvents for the polymer. Ethanol is the most used cosolvent.

A new modified RESS process, RES suspensions, has been proved successfully to coat ultrafine particles [15,16]. Coating or encapsulation of nanoparticles is a major challenge due to the extremely small size, high surface energy, and high surface area of the nanoparticles. The whole equipment consisted on a spray chamber, a supercritical extraction column and a recovery system for the particles. Before entering into the spray room, the ultrafine particles were well dispersed in the supercritical solution of coating materials to form the supercritical suspension. Silica particles of 5 μm were used as core particles. The coating material was paraffin (melting point: 48–50 °C). A nanoscale paraffin layer was deposited on the surface of silica particles. It was found that there was no significant agglomeration during coating process.

Based in the Wurster process [4], a new coating method with a fluidized bed was investigated by Tsutsumi and coworkers [17] in 1995 to process fine particles (d_p < 100 μm) and ultrafine particles (d_p < 10 μm). Due to their small size, these particles present a strong cohesivity, therefore the conventional fluidised bed coating process, which usually involves the spraying of the coating material, should not be applied to avoid agglomeration problems. This work showed a fluidized bed of 50 μm-spheroidal–catalist particles operated with air at ambient conditions. The coating agent, paraffin wax, was dissolved in SC-CO_2 and expanded through a nozzle inside the fluidized bed. The microparticles were successfully coated and the thickness of coating layer controlled by the concentration of the supercritical solution of the paraffin wax.

To get a better mixing of small particles (d_p < 100 μm), the process evolved to the use of high pressure fluidized beds ($P > P_c$) [18–21]. This was further developed and investigated by Schreiber et al. [22–24]. In their works, the performance of the coating of glass beads microparticles (d_p = 169 μm) with two paraffins with different melting and glass transition temperatures was analyzed. The operating conditions in the coating/fluidization step were kept constant at 8 MPa and 40 °C. They found that using the paraffin having the lower glass transition temperature (52 °C) near the operating temperature of the fluidized bed resulted in a high agglomeration tendency, whereas hardly any agglomeration was observed with the paraffin having the higher glass transition temperature (55 °C). The higher melting point paraffin (60 °C vs. 55 °C) also resulted in a very uniform surface coating. However, Kröber and Teipel [21] reported uniform and non-agglomerated coatings for glass beads of 70 μm with stearyl alcohol (T_m = 55 °C) in a SC-CO_2 fluidized bed at 8 MPa and 55 °C.

1.2. Mechanism in particle coating by RESS process

Particle formation by RESS process is considered in terms of initial nucleation and subsequent growth phenomena. If the RESS expansion occurs in single-solvent phase, a homogeneous nucleation, strongly dependent on the solute supersaturation degree is expected [8]. However, the presence of a previous surface (core particles) may vary this mechanism.

Besides, in the coating process, interfacial forces, viscosities as well as contact angles of the system core particle–solute–SCF come into play and influence important factors of the coating performance, such as yield, thickness and agglomeration tendency [20]. Interfacial forces and viscosities diminish when increasing pressure, whereas contact angle increase.

The thickness of the coating is mainly influenced by the wetting [20], which in turns depends on the interfacial forces between the coating material and the surrounding fluid and on the contact angle of all three apparent phases. The wetting can be considered sufficient in a coating process when the contact angle is smaller than 90° [23].

The yield of the process depends on the wetting behaviour of the solid surface, as well. It will be low if the coating material does not adhere to the core particle or solidifies before hitting the particle. The low interfacial tension of SCF and SCF solutions favours the creation of new interfaces enhancing the efficiency of the precipitation process [24]. However, the yield of the coating process may decrease due to the faster solidification of smaller droplets/particles of coating material.

The agglomeration tendency, which needs to be avoided for coating processes, is more influenced by the liquid bridges formed by the coating material than by the electrostatic forces and van der Waals forces. The strength of the liquid bridges is influenced, in one

hand, by the viscosity of the binder solution and, in the other hand, by the contact angle.

Therefore, high pressure processing reduces agglomeration due to the low viscosity and to the fact that high operation pressures increase contact angles so the static liquid bridges strength is reduced. The increase of temperature has the opposite effect on the contact angles, although it only becomes significant for porous surfaces. This feature affects also the agglomeration tendency, porous surface particles are more likely to agglomerate than smooth particles [24].

Unfortunately, there are not many studies on these measurements (interfacial forces, contact angles, and viscosities) of these sorts of systems (polymer, solid particle and SCF) at elevated pressures [25].

This coating process in a high pressure fluidized based on the RESS process is outlined as a promising technology to coat microparticles. The aim of this work is to study the influence of operational parameters of both parts of the coating process, RESS and high pressure fluidized bed, on the product yield and quality.

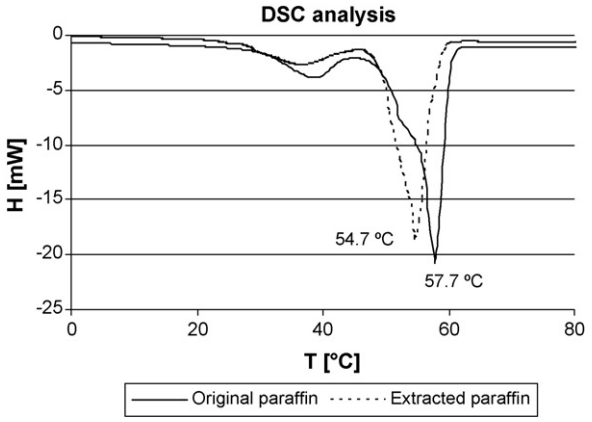

Fig. 1. DSC study of an original and processed sample of paraffin.

2. Experimental

2.1. Materials

The carbon dioxide was of 99.5% purity and was provided by S.E. Carburos Metálicos S.A. (Spain). The glass beads (GB) particles ($d_{p,s}$ = 176 μm) were purchased to Sigma–Aldrich. Glass beads were chosen because they are commonly used as model particles in many works due to their sphericity ($\phi \approx 1$) and smooth surface. The paraffin wax, characterized by melting interval of 52–54 °C, was supplied by Merck and used as received. Nevertheless a differential scanning calorimetry (DSC) analysis (Fig. 1) was made to verify the melting temperature of the paraffin (57.7 °C) and the glass transition temperature (54.7 °C).

The influence of pressure and temperature in the contact angle of the system glass beads–paraffin (T_m = 60 °C) has been investigated by Schreiber et al. [24] showing values below 70° in the studied operating range of pressure (0.1–25 MPa) and temperature (60–70 °C).

2.2. Equipment

The apparatus (Figs. 2 and 3) has been designed and tested for working at a maximum pressure of 30 MPa and temperature 100 °C. All the vessels have been evaluated by a hydrostatic pressure test according to the European Directive for pressure equipments 97/23/CE.

Two different layouts have been used to meet the demands for the bottom (Fig. 2) and top spray experiments (Fig. 3).

Basically, the set-up consists on two process vessels, the extractor (D-130) and the fluidized bed (D-140). Both process vessels have a removable basket in order to make the handling of the solid materials, packing and glass beads, easier. The baskets (V = 0.582 L; D = 40.9 mm) are made of stainless steel and have porous plates (Poral; Pore size: 1.2 microns) at bottom and top.

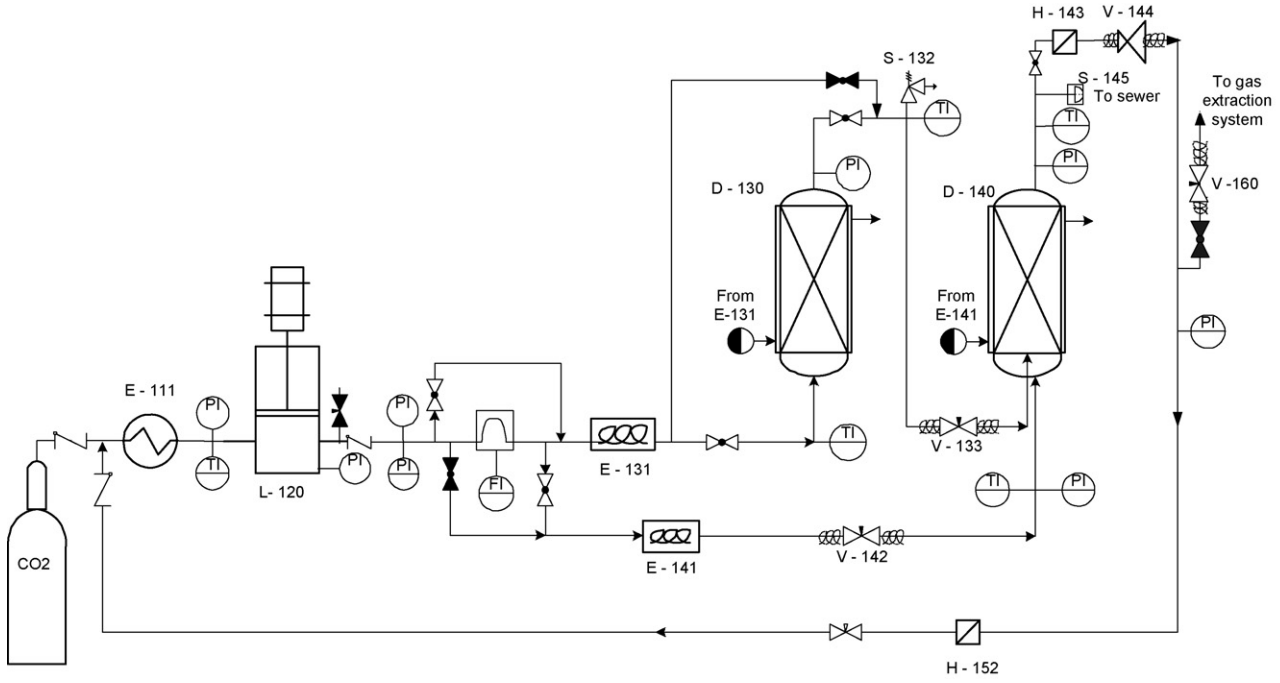

Fig. 2. Diagram of the equipment for bottom spray experiments.

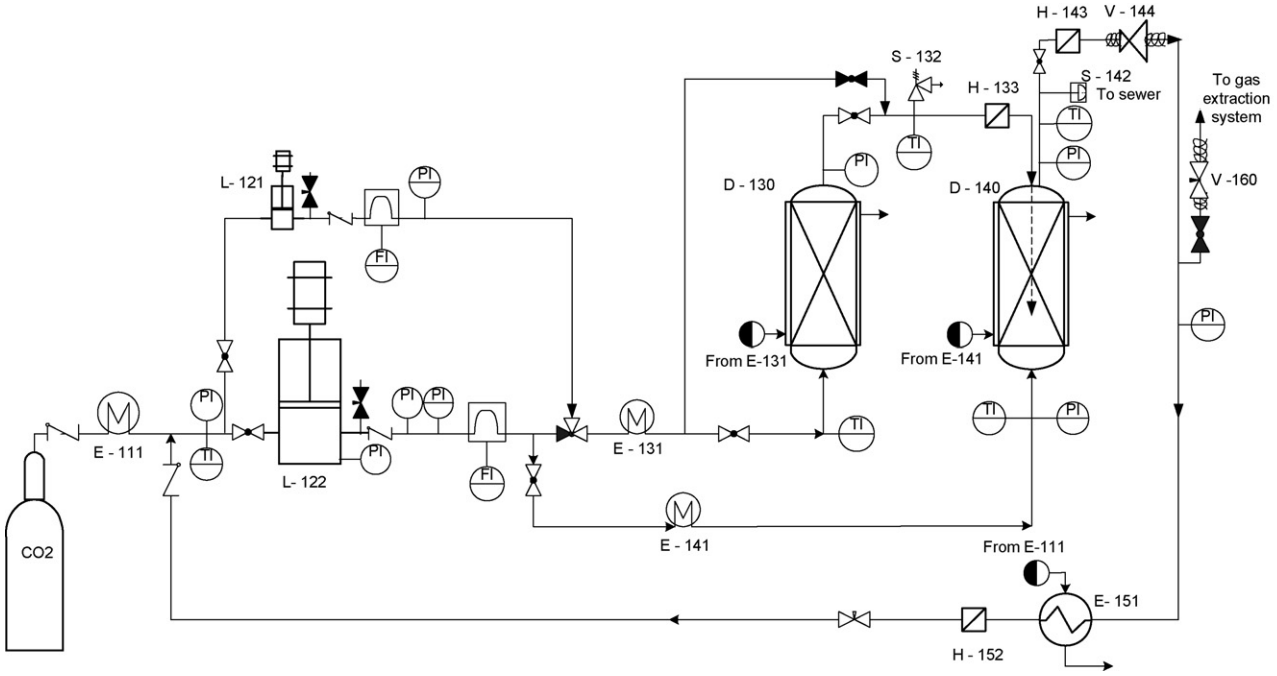

Fig. 3. Diagram of the equipment for top spray experiments.

The CO_2, stored at ca. 5 MPa, is supplied in liquid state to both steps of the process, extraction and fluidization, by high pressure membrane pump (L-122; LEWA GmbH, Germany; 30 MPa; 2–40 L/h). Previously, it is cooled down in a cryostate (E-111) to assure its liquid state and to avoid cavitation in the pump.

The CO_2 temperature in each step of the process is set up by coils submerged in thermostatic baths (E-131; E-132). The thermostated water circulates also in the jacket of the process vessels (D-130; D-140).

The pressure is adjusted by different ways in each step of the process; in the extraction step it is adjusted by the expansion device (see Section 2.2.1) and in the fluidization step, it is set by a backpressure valve (V-143; GO regulator, Mod. BP-66).

To reduce the CO_2 consumption and emissions, it is recirculated to the system at ca. 5 MPa. When the experiment finishes, the backpressure valve is completely opened and afterwards, the decompression valve (V-160) is slightly opened to relief the fluid, hence the pressure, continuously but smoothly.

In order to perform the top spray experiments (Fig. 3), a second pump (L-121; Dosapro Milton Royal, France; 30 MPa; Q_{max} = 4.79 L/h) was used to supply the CO_2 to the extraction vessel. Also, an independent cooler (E-151) was implemented in the recirculation stream, just after the pressure regulator (V-143), to reduce the deposition of paraffin all along the walls of the tubes, due to the reduction on solubility, and to produce it in this cooling device, which is easy to separate from the hole equipment and to clean with an organic solvent (hexane, ethyl-acetate). Downstream, there is an on-line filter (HOKE; Pore size: 15 microns) to check that the CO_2 to the pumping section is free of solute (paraffin).

2.2.1. Expansion device

The design of the expansion device is an essential element of the process equipment in a RESS process. It is inside this piece where the expansion of the coating solution takes place; consequently it controls either the pressure inside the extraction vessel (D-130) or the flow rate of coating solution to be expanded.

In this work two different elements have been tested. In a first set of experiments, the saturated solution from vessel D-130 was introduce at the bottom of the fluidized bed by means of a 1/8 in. tubing and the pressure drop was produced in a micro-metering valve (V-133). This valve was located before the 1/8 in. tubing next to the inlet of the saturated stream into the fluidized bed. This configuration (Fig. 2) allowed setting extraction pressure independently from the fluidized bed pressure.

Due to different operation problems that will be explained in detail in Section 3, the top spray arrangement shown in Fig. 3 was proposed.

In the set of top spray experiments, homemade nozzles were used. These nozzles were constructed in a capillary tube of 1/16 outer diameter (O.D.) with two different inner diameters, 0.180 mm and 0.130 mm. They were connected to the installation tubing (1/4 in. O.D.) by a reduction piece union (Fig. 4).

The nozzle position is also important. It has to be made sure, that the flow leaving the nozzle has immediately contact with the particles to assure its liquid state. Therefore the nozzle has to be located inside the fluidizing zone of the autoclave. If the nozzle is located very low, it is probable that a part of the particles remains above the nozzle during the operation. Hence the optimal position of the nozzle is at the highest possible point inside the fluidized bed. Considering a mean porosity value of ε = 0.46 at the operating fluid velocity (1.5 u_{mf}) from the experimental values from the literature

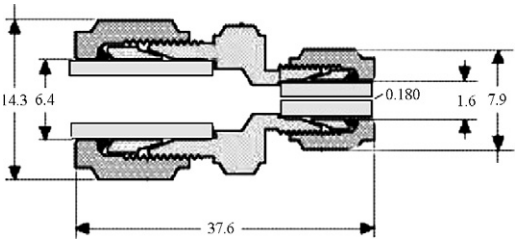

Fig. 4. Nozzle piece (dimensions in mm).

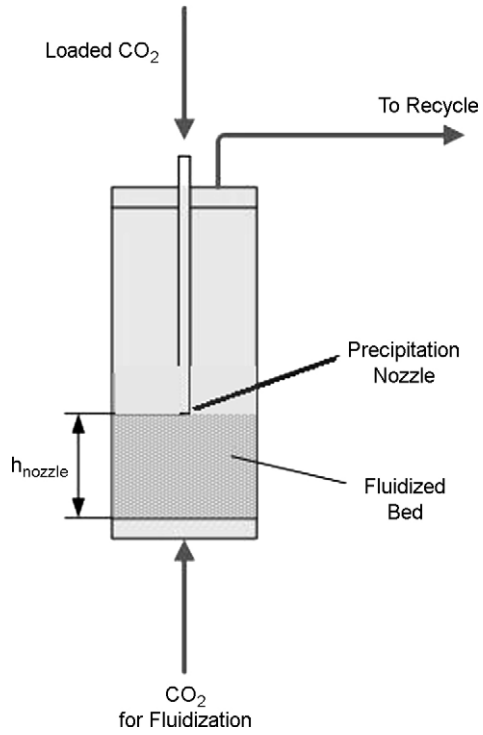

Fig. 5. Nozzle position in top spray experiments.

[21,26] at 9 MPa and 35 °C, and a solid filling of 200 g, the height of the nozzle is calculated to be h_{nozzle} = 11.3 cm (Fig. 5).

2.3. Experimental method

Before starting an experiment the basket of the autoclaves were filled with glass beads (D-140) and with the random packing (Ceramic Raschig rings, 6 mm) that carries the paraffin (D-130). The purpose of this packing is to provide a support for the paraffin in order to avoid clogging as well as to offer a good contact between the fluid (SC-CO_2) and the solute (paraffin). The paraffin is deposited onto this packing in a heated rotating flask until the paraffin is totally molten. Then it is slowly cooled down to ambient temperature, maintaining rotation.

Afterwards, the whole apparatus is put to pressure and heated, until the desired process temperature is achieved. Then, the fluidization flow is started and a flow through the nozzle is established bypassing the extraction autoclave. When all flow values are stable the nozzle flow is switched to pass through the extraction vessel and the processing time is taken.

After a certain coating time, the nozzle flow is put back to bypass the extraction stage and the process is continued for 2 min. The nozzle flow is continued to carry out all paraffin loaded CO_2 to prevent plugging of the nozzle and the fluidization flow is maintained to avoid agglomeration of the coated particles.

Afterwards, the pressure in the apparatus is slowly released and the baskets containing the filling and the glass beads are weighed.

2.4. Evaluation of the process

2.4.1. Quantitative analysis

To analyse the effect of the different operation condition tested on the coating results, several "control variables" have been defined:

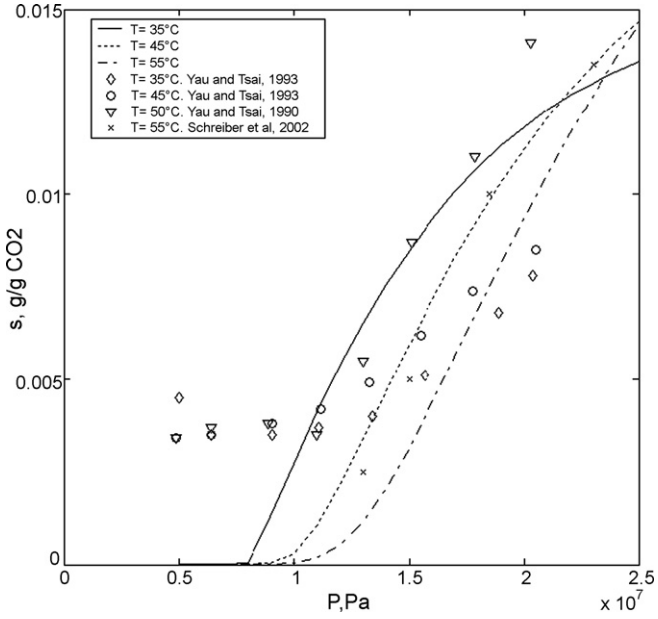

Fig. 6. Paraffin solubility in CO_2 calculated with the GC-EOS [30].

- % Global yield (η_{global}), defined as the mass of wax deposited on the particles divided by the mass of wax extracted from the extraction autoclave.

$$\%\eta_{global} = \frac{m_{coating}}{\Delta m_{extracted}} \times 100 \quad (1)$$

To determine the weight of the paraffin that actually remains on the glass beads ($m_{coating}$), a probe of the glass beads is place into an oven at 450 °C for 2 h to burn the paraffin. The difference in weight before and after the burning indicates the amount of paraffin that coated the glass beads.

The amount of extracted paraffin ($\Delta m_{extracted}$) is evaluated as the subtraction of the weight of the extraction basket before and after the experiment.

- % Extraction yield ($\eta_{extraction}$), defined as the amount of extracted paraffin ($\Delta m_{extracted}$) divided by the solubility (S) of paraffin in the operation conditions, to test whether the stream has been saturated or whether entraiment has took place.

$$\%\eta_{extraction} = \frac{\Delta m_{extracted}}{S} \times 100 \quad (2)$$

The solubility of paraffin in SC-CO_2 at the extraction conditions is taken from the literature. The system paraffin–CO_2 and n-alkanes–CO_2 has been already investigated by several researchers [22,27–29] and there are equations of state (EOS) that have been successfully used with this kind of mixture. Fig. 6 shows three solubility isotherms of the mixture calculated with the model proposed by Skjold-Jørgensen [30], an equation of state (EOS) developed for polar as well as nonpolar components. It is based on the generalized van der Waals partition function and uses local-composition mixing rules according to a specific group-contribution calculation of this equation of state (the GCEOS). The three isotherms are plotted together with experimental solubility data of a paraffin wax with the same melting point from Schreiber et al. [22] and data from the system $C_{28}H_{58}$–CO_2 measured by Yau and Tsai [27]. As it can be seen, the prediction is good for pressures between 10 and 25 MPa, having into account that it only requires information concerning readily accessible pure-component properties (critical temperature and critical diameter of the molecule). However,

Table 1
Operations conditions for the bottom spray experiments

Variable	Extraction step	Coating step/fluidization
Pressure	18–22 MPa	8–10 MPa
Temperature	35–55 °C	30–50 °C
Flow rate	0.75–2.5 kg/h	$1.25u_{mf} - 2.25\ u_{mf}$ m/s
Mass of glass beads	–	0.075–0.200 kg
Operation time	10–30 min	

it should not be applied below 10 MPa because it predicts very low values.

- % Coating yield defined as the percentage of the ratio of the mass of wax deposited on the particles ($m_{coating}$) to the total amount of paraffin in the basket; it takes into account the mass deposited also in walls or entrained that was stopped by the outlet porous disc ($\Delta m_{deposited}$).

$$\%\eta_{coating} = \frac{m_{coating}}{\Delta m_{deposited}} \times 100 \quad (3)$$

- % Wax loading (X), defined as the mass of wax deposited on the particles divided by mass of particles. This value is proportional to the coating thickness, supposing uniform coating of spherical particles.

$$X = \frac{m_{coating}}{m_{particles}} \times 100 \quad (4)$$

2.4.2. Qualitative analysis

The degree of agglomeration and the continuity and uniformity of the coating are qualitative variables, which were characterized by SEM-images of the paraffin covered glass beads. A variable pressure scanning electron microscope was used (Hitachi, S-3400N), which offers the possibility to distinguish between different substances corresponding to their electrical conductivity, since no metallization of the surface is necessary. Therefore, dark paraffin coated areas appear over the light grey glass surfaces.

3. Results and discussion

Two set of experiments have been carried out to study the coating of microparticles by means of a RESS process in a high pressure fluidized bed with two different expansion devices. Experimental conditions were varied within the ranges shown in Table 1, to investigate the most influencing parameters (temperature, pressure and flow) of the two steps of the process (extraction and coating).

The effect of the operation conditions is different in each step. In the extraction one, high pressure helps to concentrate the coating material in the CO_2 stream while high temperature decreases the solubility power. In the coating and fluidization step the pressure has two opposite effects. Regarding coating, low pressure is recommend because in this way the reduction in solubility will be more dramatic, hence more coating material will precipitate. However, high pressure enhance the fluidization quality of microparticles, hence the performance of the coating will be better.

The flow rate in the extraction stage, influence the degree of saturation of the CO_2 flow; in the coating affects the mixing of the particles, the higher the flow the greater the mixing. The working flow rate in the coating step is varied in relation to the minimum fluidization velocity, which is calculated according to the Wen and Yu equation [31]:

$$Re_{mf} = (33.7^2 + 0.0408\mathrm{Ar})^{0.5} - 33.7 \quad (5)$$

This equation has been tested successfully for high pressure fluidization in a previous work [32].

3.1. Bottom spray

The analysis of the quantitative results of this first set of experiments (Table 2) allows establishing the following general trends.

Concerning the extraction step, the solubility varies from 0.008 to 0.014 g/g for density values between 700 and 900 kg/m^3. The main parameters to get a good paraffin saturation in the CO_2 stream are time and flow rate: high flow rates and long extraction times reduce extraction yield because of the extraction basket run out of the CO_2 that has been in contact with the paraffin wax during the conditioning time, pressurization and heating, without an outgoing flow and sufficient time to saturate.

Regarding the coating step, density values below 300 kg/m^3 are necessary to achieve a good global yield of the process, which means to precipitate above 70% of the paraffin extracted in the previous step. This fact shows the importance of hydrodynamics in the RESS process, apart from the solubility, which is low enough in all the experiments, about 0.003 g paraffin/g CO_2 (Fig. 6), because the pressure is kept below 10 MPa.

The coating yield seems to be related, not only to the operation conditions but also to the total CO_2 flow: the higher the flow, the smaller the yield; a possible explanation is that precipitated paraffin is again solubilized, despite the low solubility values because of the high flow rate, and that particles of precipitated paraffin are easily entrained against basket walls and top disc, as other authors suggested in previous works [20,24].

Table 2
Experiments performed with the bottom spray equipment

#	u/u_{mf}	Extraction						Precipitation					Global process	
		P (MPa)	T (°C)	ρ (kg/m^3)	Extraction flow (kg/h)	Extraction time (min)	$\%\eta_{extraction}$	P (MPa)	T (°C)	ρ (kg/m^3)	$m_{particles}$ (g)	$\%\rho_{coating}$	X (g/g)	$\%\eta_{global}$
1	0.99	18	44	795	1.6	30	89.5	8.0	40	280	165	60.7	2.21	51.3
2	0.97	20	37	855	2.3	20	26.7	7.9	50	215	165	97.2	1.38	90.0
3	0.84	22	50	805	1.4	30	*	8.0	37	335	97	40.3	1.40	16.6
4	1.29	18	30	874	0.5	10	37.2	7.4	32	321	91	53.9	0.29	29.8
5	1.33	20	53	767	2.4	10	82.0	8.0	39	292	88	84.6	2.60	69.2
6	1.36	22	37	872	0.8	30	75.2	8.0	51	215	79	55.3	1.32	22.4
7	1.68	18	53	737	1.6	10	60.4	8.0	54	206	110	67.0	0.91	71.8
8	1.72	18	52	744	1.9	20	66.0	9.7	50	356	160	70.3	1.32	66.6
9	1.79	20	41	835	0.7	20	75.6	8.2	33	653	91	22.0	0.21	6.8
10	1.80	22	33	890	0.8	20	83.3	8.2	35	516	114	98.2	0.59	26.8
11	1.92	20	40	840	1.6	20	38.2	8.2	35	572	120	56.7	0.23	6.8
12	2.07	20	40	840	1.2	10	*	9.9	38	665	160	50.8	0.45	18.5
13	2.34	22	54	786	2.3	30	45.9	8.1	33	641	102	29.1	1.80	23.4

*Percentage values higher than 100%.

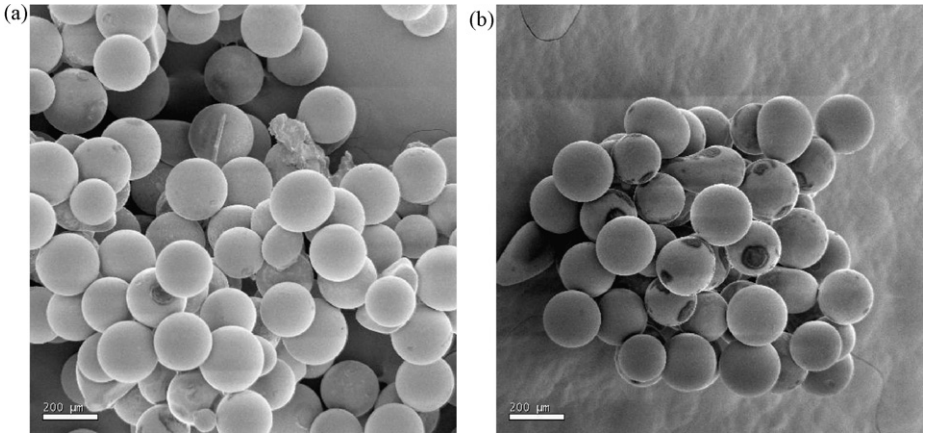

Fig. 7. Particle agglomerations: (a) Experiment #2 and (b) Experiment #10.

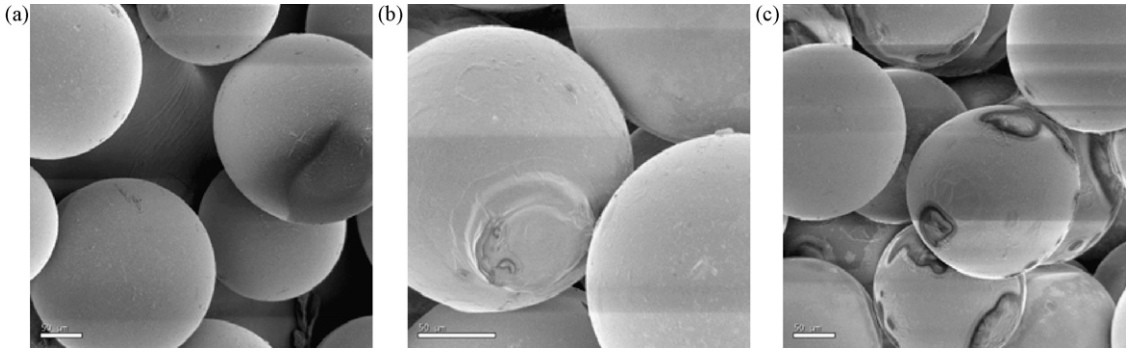

Fig. 8. Detail of uncovered (a) and covered ((b) Experiment #2 and (c) Experiment #10) glass beads.

Concerning quality aspects, the size and amount of agglomerates diminish when the ratio u/u_{mf} is increased, as expected (Fig. 7). The influence of temperature is not significant: agglomerates are found working far below the glass transition temperature of the wax (Exp. #10) as well as at close temperature (Exp. #2). SEM photographs in Fig. 8, show a detail of the coated particles: Fig. 8(b) shows a complete an uniform coating film, whereas Fig. 8(c) shows a partial coating, probably due to the low paraffin loading value ($X = 0.6$).

The main problem of this set of experiments was the control of the extraction pressure and the extraction CO_2 flow. In normal operation, the incertitude in the measure of the extraction flow was between 5% and 10%. However, sometimes this incertitude increased up to 60% of the CO_2 extraction flow due to plugging in V-133 caused by the Joule–Thompson effect in spite of being surrounded by an electrical resistance. Besides, the precipitation of paraffin already started in the entrance capillary producing agglomeration at the bottom of the bed. Consequently, the use of a valve upstream of the bed was dismissed and the new equipment configuration shown in Fig. 3 was tested.

3.2. Top spray

This new equipment configuration (Fig. 3) with a nozzle to produce the expansion of the CO_2 was developed to avoid the precipitation of paraffin before it enters to the fluidized bed. The nozzle was situated just on top of the bed (Fig. 5) to avoid the reduction on coating efficiency due to spray drying of droplets and the subsequent fines production [1].

In this second set of experiments, displayed in Table 3, the ratio u/u_{mf} was maintained at 1.5 because the maximum flow rate was limited by the cooling capacity of the concentrical cooler just after the backpressure (Fig. 3). Nevertheless, the mixing was enough to assure a uniform coating and to avoid agglomeration. In the same way, the amount of particles was set to the highest value (200 g) in all the experiments, because high quantities of solids contribute to increase the mixing in the fluidized bed [33].

The $\%\eta_{coating}$ can be consider as a good indicator of the quality of the fluidization, high values indicate that the paraffin is deposited preferably in the particles and it is not entrained with the fluidizing SC-CO_2 stream.

Table 3
Experiments performed with the top spray equipment

Nozzle length = 7 mm			Extraction							Precipitation				Global process	
#	Nozzle diameter (m)	u/u_{mf}	P (MPa)	T (°C)	ρ (kg/m^3)	Extraction flow (kg/h)	Extraction time (min)	No of intervals	$\%\eta_{extraction}$	P (MPa)	T (°C)	ρ (kg/m^3)	$\%\eta_{coating}$	X (g/g)	$\%\eta_{global}$
1	0.18	1.23	17	34	844	4.6	15	1	52.4	9.8	35	702	90.0	0.22	7.1
2	0.13	1.16	20	37	853	4.1	45	1	22.2	8.1	34	596	100.3	1.75	43.2
3	0.18	1.49	18	45	788	3.8	30	1	45.7	9.0	36	637	100.8	1.31	30.8
4	0.18	1.48	17	44	789	4.3	5	5	80.2	9.1	38	600	100.1	0.61	10.6
5	0.18	1.55	17	46	765	4.1	5	3	93.5	9.0	35	661	5.1	0.09	2.1

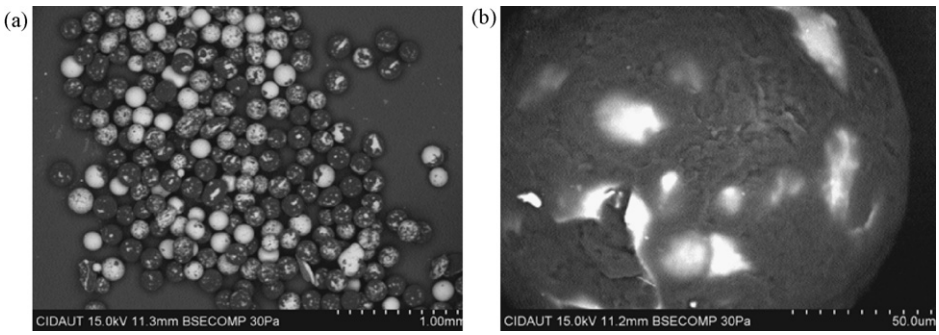

Fig. 9. Coated particles from Experiment #2: (a) general view and (b) detail (800×).

The main drawback of using a nozzle is that the extraction pressure and flow rate are determined by the dimensions of the orifice and the conditions fixed in the fluidized bed. Consequently, the extraction flow rate was too high compared to the values recommended from the previous experiments and the obtained extraction yield was smaller. Different strategies were tested in order to increase the extraction yield ($\%\eta_{extraction}$). First a longer processing time was tried (Exp. #2), but it resulted in a lower average paraffin load of the CO_2 flow, despite that the extraction pressure was higher, indicating a kinetic problem. Then, process conditions were modified. Since higher temperature improves extraction kinetics, although decreases the saturation value in CO_2, the extraction temperature was set to a 45 °C. Despite the increase in $\%\eta_{extraction}$, it was still below 50% and, hence, the paraffin was extracted in intervals. As explained before, the CO_2 contained in the extraction autoclave before starting the experiment is saturated in paraffin. Assuming plug flow behavior inside the extraction autoclave it takes about 5 min for the saturated fluid to leave. Therefore, after a 5-min interval of normal operation, the extraction flow bypassed the saturation autoclave for 15 min followed by another 5-min of extraction and so on (Exp. #4 and #5); the paraffin loading was almost doubled. Nevertheless, another problem arose, while the extraction flow was stopped, stopping also the fluidization flow of the bed resulted in agglomeration of the coated particles making the coating useless. But maintaining the fluidization resulted in extraction of the already precipitated coating by the fluidization flow leading to very low yields and insufficient coating (Exp. #4). Since the different operational strategies were not successful, alternative nozzle designs were proposed with longer capillaries or smaller diameters to raise the upstream pressure and to reduce the extraction flow rate. Unfortunately no successful experiments with a longer capillary nozzle were performed because of plugging problems.

The global yield of all the experiments is below 50%, corroborating the conclusion pointed out with the results from Table 2, that a density below 300 kg/m^3 is necessary to achieve high yield values.

The coating quality was analyzed again by means of SEM photographs, from a variable pressure equipment, where paraffin coated areas are represented in dark over the light grey color of glass surfaces.

In Fig. 9, coated particles from Exp. #2 are shown. No agglomeration tendency is observed, in contrast with results found in bottom spray experiments for similar operation conditions (Exp. #10; Fig. 7b) and confirming that the risk of agglomeration of small particles in bottom spray equipments is elevated because of the high concentration of wet particles [1]. However, the distribution of coating in the bed was not homogeneous enough, since some of the particles are almost uncovered. This indicates insufficient mixture in the fluidized bed, which was operated at only 1.16 times the minimum fluidization velocity. The covered fraction of the glass beads shows a smooth and almost intact coating layer and the sphericity of the coated glass beads still remains, which indicates that the paraffin hit the surface in liquid state and spread well before drying. The bright areas in the detail do not show uncovered areas, they are originated by the electron beam of the SEM.

The results from Exp. #4 are shown in Fig. 10: particles with little paraffin loading but a very homogeneous distribution of the coating. This indicates that the fludization velocity $u = 1.5\,u_{mf}$ was sufficiently high to provide a good agitation of the fluidized bed. Fig. 10(b) shows an early stage of coating process. The similar size of the paraffin spots on the glass beads surface and their almost circular shape indicate that the coating agent hit the surface as liquid droplets of very similar sizes. This is a hint of the good performance of the nozzle.

Another aspect to bear in mind is the change in composition of the coating material. Since paraffin is formed by a mixture of different alkanes, the shorter chained alkanes are extracted faster and therefore separated from the longer chained paraffins. To confirm this fact a DSC of the paraffin that was taken from the filter of the

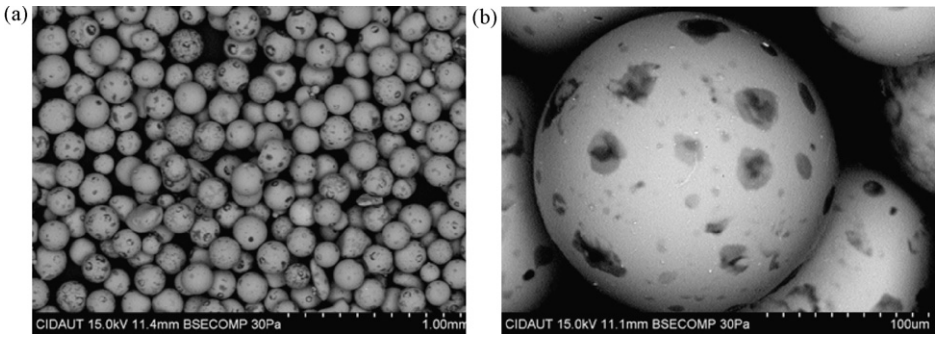

Fig. 10. Coated particles from Experiment #4: (a) general view and (b) detail (470×).

CO_2 recycle was made and compared with the DSC-profile of the original paraffin. As shown in Fig. 1, the temperature of the melting peak of the extracted paraffin is about 3 °C smaller than the corresponding temperature of the original paraffin and the glass transition temperature was reduced to 50.3 °C.

In this case, the effect has no noticeable impact on product characteristics. Nevertheless, it should be always taken into account due to the effect of polymer composition on its mechanical and physical properties.

4. Conclusions

Two series of experiments have been carried out to investigate the effect of operation conditions and equipment designs in the microparticle coating process in a high pressure fluidized bed environment.

The analysis of the operation conditions shows that a density values below 300 kg/m^3 (that means pressures below 9 MPa and temperatures above 40 °C) are necessary in the precipitation vessel to achieve a good global yield of the process, temperatures below 40 °C favour a faster solidification of the paraffin preventing the agglomeration of the particles. The pressure is slightly below of the value recommend to have good mixing in the fluidized bed, but it is imposed by the solubility of coating material. This is an important aspect: the operation conditions should be adjusted for each pair of core and coating materials, mainly depending on the solubility of the coating material in the supercritical fluid.

The extraction flow rate, according to the bottom spray of experiments, should be kept below 2 kg/h to achieve good extraction yields. However, in the top spray experiments values of 4 kg/h were employed because of the nozzle orifice size (0.180 mm O.D. and L = 7mm). In this context, the nozzle design has come out as a crucial factor to maintain or even raise the upstream pressure at a much smaller flow rate and hence, increasing retention time in the extraction step. The alternatives are longer capillaries or smaller diameters.

Concerning quality aspects, better results for equivalent operating conditions were achieved in the top spray experiments. Probably due to the small particle concentration of wet particles in the vicinity of the nozzle with regard to the bottom spray configuration. Besides, the flow rate in the fluidization/coating step should be high enough to keep fluidization velocity above 1.5 the minimum fluidization velocity (u_{mf}) to provide a good mixing and obtain a uniform distribution of the coating material in the whole bed of particles.

Acknowledgments

The authors acknowledge the financial support of this research provided by the Spanish Ministry of Education and Science (MEC) project CTQ 2006-02099. Soraya Rodríguez-Rojo thanks the MEC for her grant from the F.P.U. Program. The collaboration of Angel Martin is grateful acknowledged.

References

[1] E. Teunou, D. Poncelet, Batch and continuous fluid bed coating—review and state of the art, J. Food Eng. 53 (2002) 325–340.
[2] Ullmann's Encyclopedia of Chemical Technology. "Microencapsulation". 5th Edition CD-ROM, 1997/2001. Wiley–VCH, Weinheim. Germany.
[3] P. Kerkhof, Some modeling aspects of (batch) fluid-bed drying of life-science products, Chem. Eng. Proc. 39 (2000) 69–80.
[4] B. Guignon, E. Regalado, A. Duquenoy, E. Dumoulin, Helping to choose operating parameters for a coating fluid bed process, Powder Technol. 130 (2003) 193–198.
[5] I. Kikic, P. Sist, Applications of supercritical fluids to pharmaceuticals: controlled drug release systems, in: Proceedings of the NATO-ANSI on Supercritical Fluids: Fundamentals and Applications, 1998.
[6] J. Jung, M. Perrut, Particle design using supercritical fluids: literature and patent survey, J. Supercrit. Fluids 20 (2001) 179–219.
[7] A. Martín, M.J. Cocero, Micronization processes with supercritical fluids: fundamentals and mechanisms, Adv. Drug Deliv. Rev. 60 (2008) 339–350.
[8] D.W. Matson, J.L. Fulton, R.C. Petersen, R.D. Smith, Rapid expansion of supercritical fluid solutions: solution formation of powders, thin films, and fibers, Ind. Eng. Chem. Res. 26 (1987) 2298–2306.
[9] N. Elvassore, A. Bertucco, P. Caliceti, Production of protein–polymer microcapsules by supercritical anti-solvent techniques, in: Proceedings of the 5th International Symposium on Supercritical Fluids, 2000.
[10] E. Weidner, V. Wiesmet, Z. Knez, M. Skerget, Phase equilibrium (solid–liquid–gas) in polyethylene glycol–carbon dioxide systems, J. Supercrit. Fluids 10 (1997) 139–147.
[11] V. Pessey, R. Garriga, F. Weill, B. Chevalier, J. Etourneau, F. Cansell, Core–shell materials elaboration in supercritical mixture CO_2/ethanol, Ind. Eng. Chem. Res. 39 (2000) 4714–4719.
[12] P.G. Debenedetti, J.W. Tom, X. Kwauk, S.-D. Yeo, Rapid expansion of supercritical solutions (RESS): fundamentals and applications, Fluid Phase Equilib. 82 (1993) 311–321.
[13] K. Mishima, K. Matsuyama, D. Tanabe, S. Yamauchi, Microencapsulation of proteins by rapid expansión supercritical solution with a nonsolvent, AIChE J. 46 (2000) 857–865.
[14] K. Matsuyama, K. Mishima, K. Hayashi, H. Matsuyama, Microencapsulation of TiO_2 nanoparticles with polymer by rapid expansion of supercritical solution, J. Nanopart. Res. 5 (2003) 87–95.
[15] N. Masuda, J. Iwatuka, W. Chen, A. Tsutsumi, Nano-coating by rapid expansion of supercritical suspensions, in: Proceedings of AIChE Annual Meeting, 2001.
[16] A. Tsutsumi, M. Ikeda, W. Chen, J. Iwatsuki, A nano-coating process by the rapid expansion of supercritical suspensions in impinging-stream reactors, Powder Technol. 138 (2003) 211–215.
[17] A. Tsutsumi, S. Nakamoto, T. Mineo, K. Yoshida, A novel fluidized-bed coating of fine particles by rapid expansion of supercritical fluid solutions, Powder Technol. 85 (1995) 275–278.
[18] M. Niehaus, U. Teipel, H. Krause, W. Weisweiler, Coating of particles in a fluidized bed using supercritical carbon dioxide, in: Proceedings of the 5th Meeting on Supercritical fluids, 1998.
[19] A.K. Sunol, J. Kosky, M. Murphy, E. Hansen, J. Jones, B. Mierau, S. Sunol, Supercritical Fluid Aided encapsulation of particles in a fluidised bed environment, in: Proceedings of the 5th Meeting on Supercritical fluids, March, Nice, France, 1998.
[20] T.-J. Wang, A. Tsutsumi, H. Hasegawa, T. Mineo, Mechanism of particle coating granulation with RESS process in a fluidized bed, Powder Technol. 118 (2001) 229–235.
[21] H. Kröber, U. Teipel, Microencapsulation of particles using supercritical carbon dioxide, Chem. Eng. Proc. 44 (2005) 215–219.
[22] R. Schreiber, C. Vogt, J. Werther, G. Brunner, Fluidized bed coating at supercritical fluid conditions, J. Supercrit. Fluids 24 (2002) 137–151.
[23] R. Schreiber, B. Reinke, C. Vogt, J. Werther, G. Brunner, High-pressure fluidized bed coating utilizing supercritical carbon dioxide, J. Supercrit. Fluids 138 (2003) 31–38.
[24] R. Schreiber, C. Vogt, G. Brunner, J. Werther, Investigation of coatings produced in a high pressure fluidized bed, in: Proceedings of the 6th International Symposium on Supercritical Fluids, 2003.
[25] R. Eggers, P. Jaeger, Interfacial phenomena in supercritical processing, in: Proceedings of the 15th International Congress of Chemical and Process Engineering, 2002.
[26] C. Vogt, R. Schreiber, G. Brunner, J. Werther, Fluid dynamics of the supercritical fluidized bed, Powder Technol. 158 (2005) 102–114.
[27] J.-S. Yau, F.-N. Tsai, Solubilities of heavy *n*-paraffins in subcritical and supercritical carbon dioxide, J. Chem. Eng. Data 38 (1993) 171–174.
[28] F. Bordet, J.-P. Passarello, T. Chartier, R. Tufeu, J.F. Baumard, Modelling solutions of hydrocarbons in dense CO_2 gas, J. Eur. Ceram. Soc. 21 (2001) 1219–1227.
[29] T. Chartier, E. Delhomme, J.F. Baumard, P. Marteau, P. Subra, R. Tufeu, Solubility, in supercritical carbon dioxide, of paraffin waxes used as binders for low-pressure injection molding, Ind. Eng. Chem. Res. 38 (1999) 1904–1910.
[30] S. Skjold-Jørgensen, Gas solubility calculations. II. Application of a new Group-contribution equation of state, Fluid Phase Equilib. 16 (1984) 317–351.
[31] C.Y. Wen, Y.H. Yu, A generalized method for predicting the minimum fluidization velocity, AIChE J. 12 (1966) 610–613.
[32] S. Rodríguez-Rojo, M.J. Cocero, High pressure fluidized bed technology applied to microparticles coating, effect of operation conditions, in: Proceeding of the 7th International Symposium on Supercritical fluid, Orlando, USA, 2005.
[33] S. Rodríguez-Rojo, N. López-Valdezate, M.J. Cocero, Residence time distribution studies of high pressure fluidized bed of microparticles, J. Supercrit. Fluids 44 (2008) 433–440.